PROCEEDINGS OF SPIE

SPIEDigitalLibrary.org/conference-proceedings-of-spie

Development of virtual reality walking collision detection test on head-mounted display

Alex Hwang, Eli Peli, Jae-Hyun Jung

Alex D. Hwang, Eli Peli, Jae-Hyun Jung, "Development of virtual reality walking collision detection test on head-mounted display," Proc. SPIE 12449, Optical Architectures for Displays and Sensing in Augmented, Virtual, and Mixed Reality (AR, VR, MR) IV, 124491J (16 March 2023); doi: 10.1117/12.2647141

SPIE.

Event: SPIE AR | VR | MR, 2023, San Francisco, California, United States

Development of Virtual Reality Walking Collision Detection Test on Head-mounted display

Alex D. Hwang, Eli Peli, Jae-Hyun Jung*

Schepens Eye Research Institute of Massachusetts Eye and Ear, Department of Ophthalmology, Harvard Medical School, Boston, MA, USA 02114

ABSTRACT

Detecting and avoiding collisions during walking is critical for safe mobility. To determine the effectiveness of clinical interventions, a realistic objective outcome measure is needed. A real-world obstacle course with moving hazards has numerous limitations (e.g., safety concerns of physical collision, inability to control events, maintaining event consistency, and event randomization). Virtual reality (VR) platforms may overcome such limitations. We developed a VR walking collision detection test using a standalone head-mounted display (HMD, Meta Quest 2) with the Unity 3D engine to enable subjects' physical walking within a VR environment (i.e., a busy shopping mall). The performance measures focus on the detection and avoidance of potential collisions, where a pedestrian may (or may not) walks toward a collision with the subject, while various non-colliding pedestrians are presented simultaneously. The physical space required for the system was minimized. During the development, we addressed expected and unexpected hurdles, such as mismatch of visual perception of VR space, limited field of view (FOV) afforded by the HMD, design of pedestrian paths, design of the subject task, handling of subject's response (detection or avoidance behavior), use of mixed reality (MR) for walking path calibration. We report the initial implementation of the HMD VR walking collision detection and avoidance scenarios that showed promising potential as clinical outcome measures.

Keywords: Virtual reality, head-mounted display, walking simulator, mobility test, collision, mixed reality, field of view

1. INTRODUCTION

Detecting and avoiding collisions during walking are critical for everyday safe mobility. Pedestrian-to-pedestrian (P2P) collisions that occur in a crowded area like busy shopping malls or transportation terminals are such cases, where not only the walking subject but also the other approaching pedestrian fail to notice a possible collision with each other. For patients with visual field loss, such type of collisions has been reported as one of their frequent mobility problems in daily life.[1-6] For patients with peripheral field loss, P2P collision occurs due to a lack of situational awareness caused by the limited visual field.

Various clinical interventions using prism glasses[7-11] and head-mounted displays[12-14] have been developed to reduce such collision risks in patients with field loss, and their efficacy has been demonstrated by visual field measure and in obstacle courses as mobility performance.[15-20] However, most obstacle courses are composed of stationary obstacles, which may be sufficient for testing navigation and path finding but do not address dynamic obstacles such as P2P collision risk. In order to claim the effectiveness of clinical interventions, they should be directly tested with P2P collision events in a realistic environment, where multiple non-colliding pedestrians are simultaneously presented along with a colliding pedestrian. However, including such dynamic/walking pedestrians in the real-world obstacle course is hard to achieve because all pedestrians need to be controlled precisely on their appearing timing, where their walking paths and speeds need to be varied event by event. Also, the P2P collision event increases safety concerns of physical harm due to a collision between the subject and pedestrians. Previously, a video-based collision detection test was developed,[21-23] showing first-person perspective walking videos to a standing subject on a large screen with a guided fixation. However, this setup did not support physical walking and thus lacked critical clues utilized in natural walking (e.g., gaze movement, depth, and locomotive sensory cues) and collision avoidance (e.g., speed and path changes).

*Jaehyun_Jung@meei.harvard.edu; phone 1 617-912-2525; https://junglab.meei.harvard.edu

Optical Architectures for Displays and Sensing in Augmented, Virtual, and Mixed Reality (AR, VR, MR) IV,
edited by Bernard C. Kress, Christophe Peroz, Proc. of SPIE Vol. 12449, 124491J

To build realistic P2P collision scenarios in a risk-free environment and overcome the limitations of real-world obstacle courses, we develop an HMD VR walking collision detection and avoidance test. Since P2P collision events are presented in a VR world while subjects walk in a real-world empty (i.e., obstacle free) space, no physical harm is posed to the subjects when they fail to detect or avoid a collision with VR pedestrians. The freedom of walking behavior (e.g., speed and path changes) and gaze movement enables to measure of realistic collision detection and avoidance performance. Also, a variety of walking environments (e.g., busy shopping mall or train station), walking paths, and collision events can be easily configured to reduce the training effects caused by repeated exposures to the same walking path which is one of the major limitations in real-world obstacle courses. This freedom of configuration also allows repeated measure data collection events. Precise event controls are another benefit afforded by HMD VR pedestrian walking scenarios where each collision event representing different types of P2P collision can be simulated with a slight variation of non-colliding (distracting) pedestrian configurations. Non-colliding pedestrians have their own randomness in their appearing position, walking speeds, and walking path, while they do not interfere the colliding pedestrian's walking path relative to the subject's walking path, e.g., non-colliding pedestrians are programmed not to block the colliding pedestrian. Finally, the subject's and pedestrians' exact positions and orientation in the VR world, the number of collisions, gaze movements, and the subject's response are logged so that the complex subject's behavior interactions with other pedestrians can be analyzed later determining the detection and avoidance of potential collisions.

2. DEVELOPMENT OF HMD VR WALKING COLLISION DETECTION TEST

2.1 Calibrating physical space requirement for experiment

The HMD VR walking experiment needs an empty space because the subject's physical locomotion needs to be allowed to measure more realistic walking performance and behaviors. However, we cannot afford the same size of such a large space used in the VR world (e.g., a busy shopping mall). To minimize the physical space requirement, we apply a "Walk-and-Turn" strategy in our test. With this strategy, the subject is supposed to walk along a straight path in the real world, while a collision (or non-collision) event is simulated in VR. Once the subject reaches the end of the path, the program asks the subject to turn 180° to face the physical path that the subject just followed. The next event in a different location of the VR shopping mall is simulated while the subject is following in reserve the same real-world path again. In our scenario design, the simulation of a collision event takes about 6s. Adding a couple of seconds before and after a collision event simulation requires about 10s of total walking time, which is about 10m of walking distance when we assume that the subject's walking speed is 1m/s on average. Since our pilot data showed that subjects need less than ±1 m of lateral space to make a natural collision avoidance behavior, our VR collision performance measuring platform can be deployed in around 2 m×10 m real-world space, which is similar to a wide corridor. Note that the subjects do not need that much lateral space because a slight change of their walking orientation or walking speed (e.g., a brief pause of walking), or both (e.g., sidestep), can avoid the pre-programmed collisions.

In this strategy, making the subjects turn exactly 180° is critical because if it fails, the subjects will deviate from the physical path and may hit the walls or any physical obstacles initially off from the path in the real-world corridor. To resolve this problem, we utilized a mixed reality (MR) technique to realign the walking path in the real world and virtual world. When the subjects arrive at the endpoint of the walking path, the HMD's view turns from VR to MR mode (i.e., passthrough view in Meta Quest 2) and asks the subjects to recalibrate their position and orientation to the predefined real-world path. Figure 1 shows an example of the MR calibration step, where a virtual calibration target (i.e., a yellow vertical line) is presented over an edge-enhanced real-world view. Subjects need to align the calibration target to the predefined (obstacle free) walking path in the real world. This MR view is also activated when subjects approach too close to possible a real-world obstacle (e.g., wall or column). To assure the safety of the subjects, our protocol requires the presence of two experimenters to monitor and prevent any possible real-world collision or tripping.

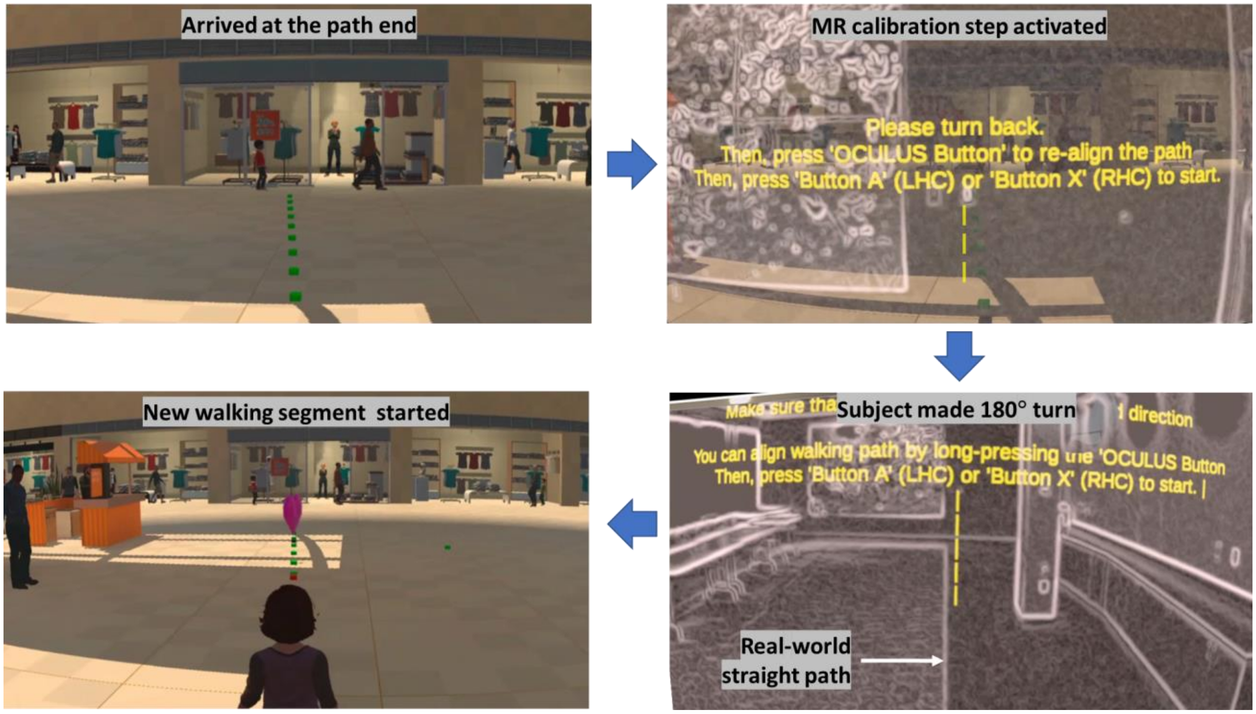

Figure 1. MR calibration steps. When subjects arrive at the VR path-end, a virtual calibration target (i.e., a yellow vertical line) is presented over an edge-enhanced real-world view (edge-filtered passthrough view in Meta Quest 2). Subjects turn 180° and then align the virtual calibration target (yellow vertical line) with the real-world (obstacle free) walking path on the floor. New segment of simulated walking starts when a subject is ready.

2.2 Measuring the FOV of the VR headset

Although the FOV of the VR HMD that we use (Meta Quest 2) was (roughly) described in their specification (~110°), we noticed that it may vary with the back vertex distance of the individual user. It is particularly important in our HMD VR walking test because the HMD itself may restrict the subject's peripheral visual field and lead to a wider head scanning pattern. Note that people with normal vision have about 180° lateral binocular visual field. In this case, a failure of collision detection approaching from the out of FOV may be due to the HMD's hardware limitation, rather than the subject's natural FOV or scanning during walking. Therefore, we needed to measure individual FOV on HMD before the task.

We developed a FOV measuring program that shows a longitudinal (for horizontal FOV) or latitudinal line (for vertical FOV) on a sphere centered at the subject's viewpoint and slowly moves (1°/s) from the far periphery to the center of the HMD's view in a VR world (Fig. 2). Subject's task was to maintain the fixation at the center of the screen and press the button as quickly as possible when the line is visible. The angular position of the line at the time of the subject's response was recorded as the FOV. The measurements were repeated to find the upper, lower, left, and right boundaries of the FOV that HMD provides. We measured the FOV of 8 normal vision subjects when they wore the HMD (Fig. 2c), which shows the variability of FOV across the subjects. We included the FOV measure before conducting the VR walking experiment to justify the effect of FOV on the detection and avoidance performance.

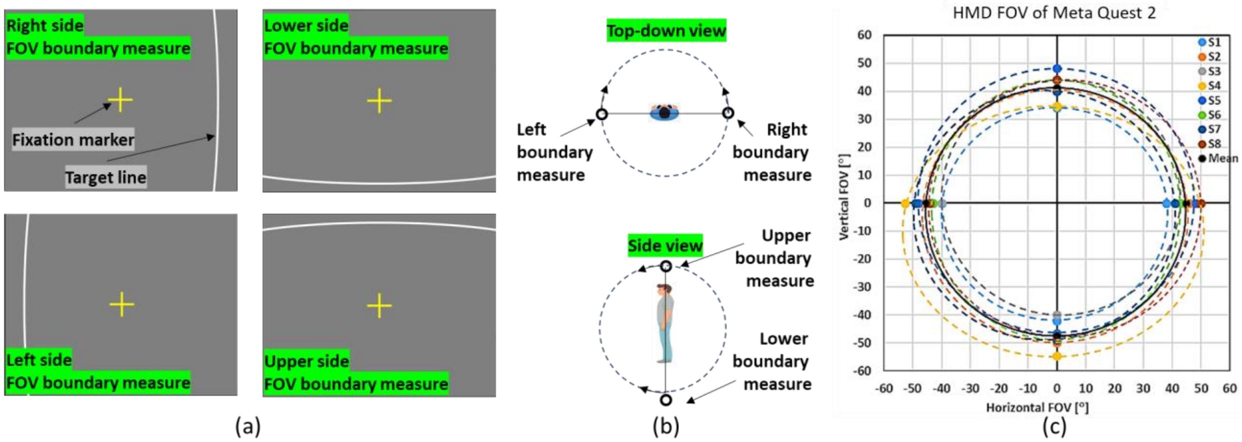

Figure 2. Individual binocular FOV measure on HMD. (a) Subject's view of the FOV measure on each side. (b) Concept of the FOV measure in top and side view. (c) Results of 8 normal vision subjects' FOV on Meta Quest 2. Note that only sizes of FOV on four axes were measured. The dashed lines are a rough estimation of FOV to connect them.

2.3 Mechanisms for events triggering and end of trial notification

Our HMD VR walking collision detection test allows the subject's free path planning during the walking. Although there is a visible path in the simulated VR world, there is no guarantee that the subject is on the path at a given time point during walking because the subject may need to be off from the path to avoid a collision. This means that at the end of the segment walk, there is no guarantee that the subject is at the end of the pre-planned path. One way to handle this issue is to put a set of visible path markers (e.g., a pink object in Fig. 1 lower-left screenshot) along the path, one for event trigger and the other for the end of path notification, and then ask subjects that they must pass through those makers at the end of the walking. However, this additional enforcement may prime the subject's response to the collision event and disrupt natural collision avoidance behavior. To minimize this problem, we set an invisible zone for event triggering and end of trial notification. When a new walking segment is started, the subject is set to stand in the invisible zone (turn off). As the subject starts walking out of the zone, a collision event is triggered (turn on), presenting various pedestrians on the scene. When the subject has walked into the zone passed the collision point, the end of the segment is initiated, which includes clearing the scene and activating the MR calibration step (Fig. 1) for the next trial.

2.4 Designing various types of collision events in VR

We designed and implemented two kinds of colliding pedestrians, *Face-to-Face* and *Overtaken* colliding pedestrians, and various *non-colliding* pedestrians serving to create a busy shopping mall environment, with the assumption that subjects are going to walk at their PWS while walking along the straight path.

<u>*A Face-to-Face colliding pedestrian*</u> appears at a given bearing angle (β) at the same distance as the subject is located from the assumed collision point when the event is triggered. The assumed collision point along the path is decided for each event, based on each subject's PWS and a designed time-to-collision (6s). For example, if a subject's measured PWS is 1 m/s and the time-to-collision is set to 6 s, the assumed collision point will be set at 6m away from the event triggering point. The colliding pedestrian is set to walk at the same speed as the subject's PWS. Since the subject and the colliding pedestrian start walking at the same distance away from the assumed collision position and at the same walking speed, they arrive at the assumed collision point at the same time, causing the collision. Figure 3a shows a *Face-to-Face* colliding event for a patient with right homonymous hemianopia (i.e., loss of field of vision in right hemifield in both eyes). The bearing angle of the *Face-to-Face* colliding pedestrian is randomly chosen among ±20° and ±40° for each event.

<u>*An Overtaken* colliding pedestrian</u> appears along the bearing angle (β) where the subject's initial position is located slightly beyond the border of the pedestrian's normal FOV (α>90°) (Fig. 3b). Since overtaken pedestrians appear in front of the subject, where the position is closer to the collision point, they walk slower than subject's PWS. Note that in a Face-to-Face colliding event, where the approaching subject is within the pedestrian's FOV (α<90°), the pedestrian may be able to detect and avoid a possible collision with the subject. In an Overtaken colliding event, however, the subject is

out of the normal pedestrian's FOV (α>90°), which means that the social responsibility to detect and avoid a possible collision is on the subject. As shown in Fig. 3b, if the subject is right homonymous hemianopia (i.e., loss of field of vision in right hemifield in both eyes), *Overtaken* colliding event may not be detected by the patient. The bearing angle of the *Overtaken* colliding pedestrian is randomly chosen among ±20°, ±40°, and ±60° for each event. Note that the colliding pedestrians with ±60° bearing angle are positioned out of the FOV afforded by the HMD (Fig. 2c), so subjects require a head scan to detect a possible collision.

Non-colliding pedestrians appear at various locations when the event is triggered. They are set to pass the assumed collision point with a randomly selected passing offset when the subject arrives at the assumed collision point (Fig. 3c). Note that the passing offset must be large enough to be clearly distinguishable from the colliding pedestrian. If the passing offset is positive, the pedestrian crosses the subject's walking path in front of the subject. If the passing offset is negative, the pedestrian crosses the subject's walking path behind the subject. The walking speed of the pedestrian with a positive or negative passing offset is set to be faster or slower than the subject's PWS, respectively. If a non-colliding pedestrian's walking path intersects with the line of sight from the subject and the colliding pedestrian during the walking, a such pedestrian is configured not to be deployed in colliding events.

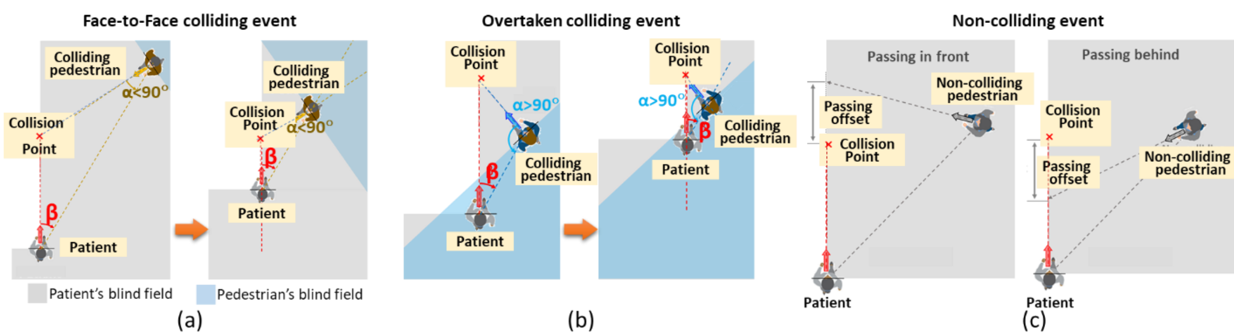

Figure 3. Design of colliding and non-colliding event for a patient with right homonymous hemianopia (i.e., loss of right half of vision). (a) Face-to-face pedestrian collision, (b) overtaken pedestrian collision, and (c) non-colliding pedestrians (passing in front and passing behind). Angle β represents the bearing angle of the pedestrian with respect to the patient's walking direction, and α represents the bearing angle of the patient with respect to the pedestrian's walking direction. Grey and blue colored fields represent the patient's and pedestrian's blind field, respectably. Note that in all conditions illustrated above, a pedestrian is approaching from the patient's blind side so without active gaze movement towards their blind side or the help of visual aids, the patients may not detect a possible collision. It may be more critical for the overtaken colliding event because not only the patient but also the pedestrian cannot notice the possible collision (α>90°).

2.5 Designing scenarios for HMD VR walking collision detection and avoidance

We provided various control options for the scenarios: turning on/off a leading kid to guide the walking speed and attention to the path and turning on/off non-colliding pedestrians to control difficulty. As a result, we developed 8 different types of scenarios: 1) No pedestrians, with a leading kid; 2) No pedestrians with no leading kid; 3) Single colliding pedestrian with a leading kid; 4) Single colliding pedestrian with no leading kid; 5) Multiple non-colliding pedestrians with a leading kid; 6) Multiple non-colliding pedestrians with no leading kid; and 7) Main scenario with a leading kid; and 8) Main scenario with no leading kid.

The first scenarios without a leading kid and without any other pedestrians (i.e., empty mall) are used to measure the subject's PWS, which is used to design individualized collision scenarios. Then the leading kid in other scenarios walks at the measured PWS which helps the subject maintain a constant walking speed. The next two scenarios with a single colliding pedestrian without any other non-colliding pedestrians were used to demonstrate the collision event and help the subject to learn the task for the experiment (e.g., press the button when they detect a possible collision and avoid it naturally while walking in VR). The run of the multiple non-colliding pedestrian scenarios without the colliding pedestrian provides baseline walking behavior (including head scanning pattern) when a subject is exposed to a heavy pedestrian traffic environment. The main scenarios are composed of all variations of colliding events in multi-pedestrian conditions (2×face-to-face collision events with bearing angles of ±20°and ±40, 2×overtaken collision events with bearing angles of ±20°, ±40°, and ±60) and 12 no-colliding (null) events which serve as catch trials (37.5% of events in a scenario). The order of each event type and the places where the event occurs are randomly assigned so that no same scenario can be experienced in the repeated scenario runs.

Figure 4. Snapshots of colliding events in action. Colliding pedestrians are marked by yellow dashed ellipses which are not part of the actual scenario. During a collision event, the colliding pedestrian remains at the same visual angle and is looming if the subject does not make any head/eye rotation and walk straight at a constant speed during walking. However, such a case hardly occurs in HMD based VR walking scenarios.

2.6 Subject task and auditory feedback design for natural interaction

The subject's task is to press a button on the left- or right-hand controller (if the subject is capable of operating two controllers), or sway a thumb stick to left or right (if the subject is not capable of handling the controller with both hands), to indicate the direction where a colliding pedestrian coming from as quickly as possible while walking naturally following the leading kid or the path indicator on the floor while avoiding a possible collision.

To maintain the subject's walking speed close to the measured PWS, auditory feedback has been added in the case subject walks too slower ("Hurry up") or too faster ("Slow down") than the measured PWS Also, to encourage the collision avoidance behavior, auditory feedback ("Hey!") is programmed to be generated if the subject approaches too close to any pedestrian (<0.5m) presented in the scene (regardless of colliding and non-colliding). The HMD walking environment for the pilot study was completed by adding a graphical user interface for user information gathering (e.g., eye height, PWS, subject ID, etc.) and scenario-to-run selection. Note that the collision event design is based on the subject's PWS, while rendering of the VR scene is based on the physical eye-height parameter so that the rendered VR scene is matched with the actual subject's eye height.

3. VISUALIZATION OF THE RESULTS

We tested our HMD VR walking collision detection and avoidance test. The proposed tool could measure various collision detection and avoidance behavior. Figure 5 shows real-world walking, corresponding HMD VR walking collision detection and avoidance test, and bird eye view with head rotation for visualization of the scenario. When the subject was walking in the real-world corridor (first column in Fig. 5), the corresponding VR shopping mall and various pedestrians were displayed on the HMD (second column in Fig. 5). The subject's response in the detection of the colliding pedestrian (second row in Fig. 5) and followed collision avoidance behavior were measured (third row in Fig. 5). Figure 6 shows vertical head rotation and walking speed changes as additional behavioral data in the subject's collision detection and avoidance while walking. Both visualizations indicate that the subject detected a possible colliding pedestrian with right head scanning (Fig. 5) at 2.87 s after the start of the trial (purple dashed line in Fig. 6). The subject first slowed down the speed (Fig. 6) and then changed the path toward the right (Fig. 5) to avoid the collision.

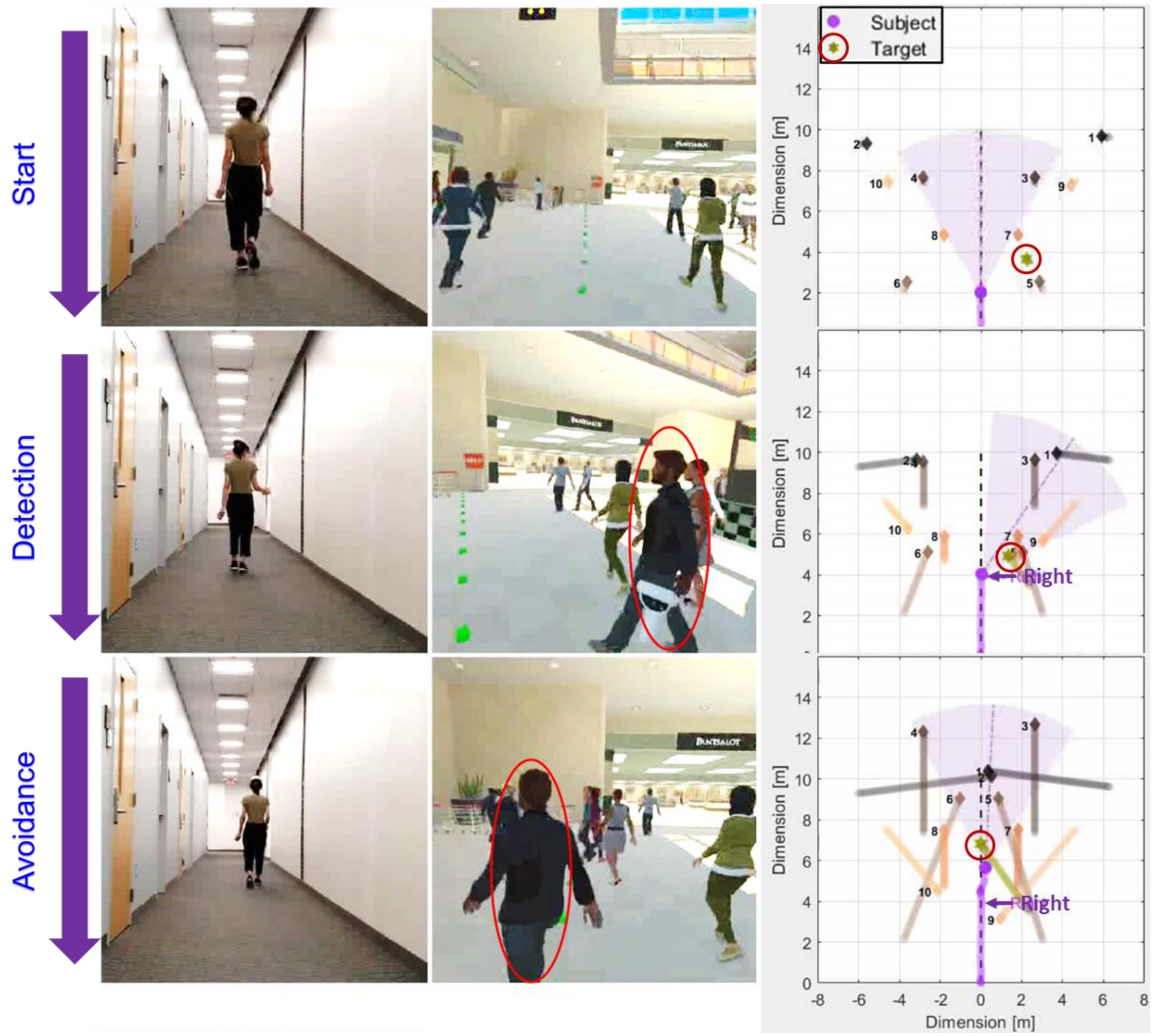

Figure 5. Example of HMD VR walking collision detection and avoidance test. While the subject was walking on a real-world empty corridor (first column), the HMD (second column) showed the busy shopping mall with various pedestrians and one colliding pedestrian (red ellipse). The detection of the colliding pedestrian, head rotation, and collision avoidance behavior were recorded. A bird-eye view visualization illustrated for logged data (third column). The FOV limited by the HMD and the subject's head orientation is represented by a purple cone shape with a dotted line. Non-colliding pedestrians' position and their walking paths are shown as various colors of diamonds with tails. The colliding target pedestrian is marked as a green star. The subject's button response (i.e., right in this trial) is shown in which direction the subject indicated. The trajectory of the subject (purple solid line) indicates the path changes of the subject to avoid collision.

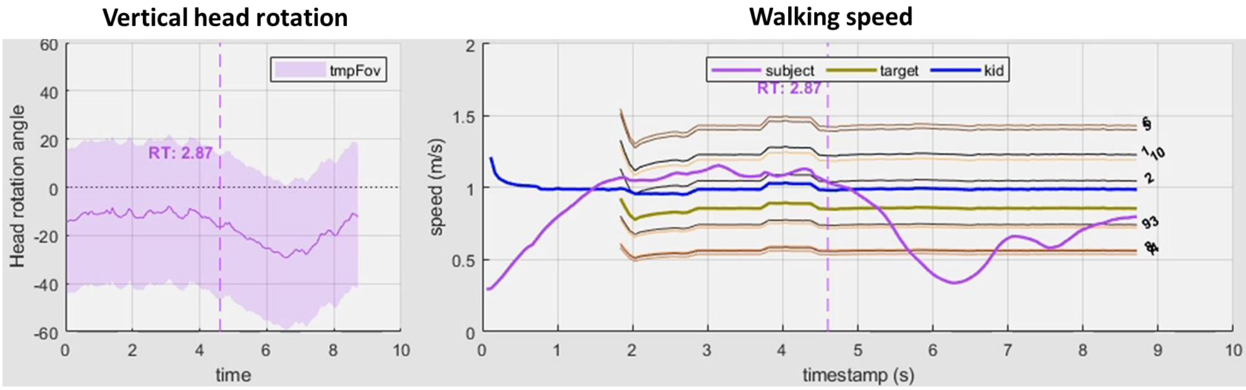

Figure 6. Visualizations of vertical head rotation and walking speed variation during the trial in Fig. 5. Purple dashed line indicates the response time (RT: 2.87 s) from the beginning of the event. The head rotation data shows that the subject looked down about 20° before detecting the possible collision, then made abrupt head rotation changes while avoiding the collision. The walking speed data shows the speed change after the detection to avoid collision. Note that the subject reached his/her PWS within 2s (=walking speed of the kid). Other non-colliding pedestrians' walking speed is also illustrated (each number represents the pedestrians in Fig. 5).

4. CONCLUSION

We developed the realistic collision detection and avoidance test on HMDs with actual walking and free gaze scanning. The result of a pilot test and data visualization utilizing the developed system showed promising potential for clinical outcome measures of walking performance in VR. We are conducting a study with normal vision and field loss patients, which includes a simulation of vision aids in VR. A validation study for our testing platform is also planned in near future.

ACKNOWLEDGMENTS

This work was supported by NIH R01EY031777.

REFERENCES

[1] Turano, K. A., Geruschat, D. R., Stahl, J. W., and Massof, R. W. Perceived visual ability for independent mobility in persons with retinitis pigmentosa. *Investigative Ophthalmology & Visual Science 40*, 865-877 (1999).

[2] Geruschat, D. R., and Turano, K. A. Connecting research on retinitis pigmentosa to the practice of orientation and mobility. *Journal of Visual Impairment & Blindness 96*, 69–85 (2002).

[3] Sugawara, T., Hagiwara, A., Hiramatsu, A., Ogata, K., Mitamura, Y., and Yamamoto, S. Relationship between peripheral visual field loss and vision-related quality of life in patients with retinitis pigmentosa. *Eye (Lond) 24*, 535-539 (2010).

[4] Lisboa, R., Chun, Y. S, Zangwill, L. M, Weinreb, R. N, Rosen, P. N, Liebmann, J. M, and Medeiros, F. A. Association between rates of binocular visual field loss and vision-related quality of life in patients with glaucoma. *JAMA ophthalmology 131*, 486–494 (2013).

[5] Lovie-Kitchin, J., Mainstone, J., Robinson, J., and Brown, B. What areas of the visual field are important for mobility in low vision patients? *Clinical Vision Sciences 5*, 249–263 (1990).

[6] Peli, E., Apfelbaum, H., Berson, E. L., and Goldstein, R. B. The risk of pedestrian collisions with peripheral visual field loss. *Journal of Vision 16*, 5 (2016).

[7] Peli, E. 2017 Charles F. Prentice Award Lecture: Peripheral Prisms for Visual Field Expansion: A Translational Journey. *Optometry and Vision Science*. *97:833–846* (2020).

[8] Somani, S., Brent, M. H., and Markowitz, S. N. Visual field expansion in patients with retinitis pigmentosa. *Canadian journal of ophthalmology 41*, 27-33 (2006).

[9] Jung, J-H., and Peli, E. Field Expansion for Acquired Monocular Vision Using a Multiplexing Prism. *Optometry and Vision Science 95*, 814-828 (2018).

[10] Choi, H-J., Peli, E., Park, M., and Jung, J-H. Design of 45° periscopic visual field expansion device for peripheral field loss. *Optics Communications 454*, 124364 (2020).

[11] Qiu, C., Jung, J-H., Tuccar-Burak, M., Spano, L., Goldstein, R., and Peli., E. Measuring pedestrian collision detection with peripheral field loss and the impact of peripheral prisms. *Transl Vis Sci Technol 7*, 1 (2018).

[12] Trese, M. G., Khan, N. W., Branham, K., Conroy, E. B., and Moroi, S. E. Expansion of severely constricted visual field using Google Glass. *Ophthalmic Surgery, Lasers and Imaging Retina 47*, 486-489 (2016).

[13] Ehrlich, J. R., Ojeda, L. V., Wicker, D., Day, S., Howson, A., Lakshminarayanan, V., and Moroi, S. E. Head-mounted display technology for low-vision rehabilitation and vision enhancement. *American journal of ophthalmology 176*, 26-32 (2017).

[14] Sayed, A. M., Kashem, R., Abdel-Mottaleb, M., Roongpoovapatr, V., Eleiwa, T. K., Abdel-Mottaleb, M., Parrish II, R. K., and Shousha, M. A. Toward Improving the Mobility of Patients with Peripheral Visual Field Defects with Novel Digital Spectacles. *American journal of ophthalmology 210*, 136-145 (2019).

[15] Soong, G. P., Lovie-Kitchin, J. E., and Brown, B. Does mobility performance of visually impaired adults improve immediately after orientation and mobility training? *Optometry and Vision Science 78*, 657-666 (2001).

[16] Leat, S. J., and Lovie-Kitchin, J. E. Measuring mobility performance: experience gained in designing a mobility course. *Clin Exp Optom 89*, 215-228 (2006).

[17] Fuhr, P. S., Liu, L., and Kuyk, T. K. Relationships between feature search and mobility performance in persons with severe visual impairment. *Optometry and Vision Science 84*, 393-400 (2007).

[18] Roentgen, U. R., Gelderblom, G. J., and de Witte, L. P. The development of an indoor mobility course for the evaluation of electronic mobility aids for persons who are visually impaired. *Assistive Technology 24*, 143-154 (2012).

[19] Patel, I., Turano, K. A., Broman, A. T., Bandeen-Roche, K., Munoz, B., and West, S. K. Measures of visual function and percentage of preferred walking speed in older adults: the Salisbury Eye Evaluation Project. *Invest Ophthalmol Vis Sci 47*, 65-71 (2006).

[20] Roentgen, U. R., Gelderblom, G. J., and de Witte, L. P. User evaluation of two electronic mobility aids for persons who are visually impaired: A quasi-experimental study using a standardized mobility course. *Assistive Technology 24*, 110-120 (2012).

[21] Qiu, C., Jung, J-H., Tuccar-Burak, M., Spano, L., Goldstein, R., Peli, E. Measuring Pedestrian Collision Detection With Peripheral Field Loss and the Impact of Peripheral Prisms. *Translational Vision Science & Technology*, 7: 1 (2018).

[22] Jung, J-H., Castle, R., Kurukuti, N. M., Manda, S., Peli, E. Field Expansion with Multiplexing Prism Glasses Improve Pedestrian Detection for People with Acquired Monocular Vision. *Translational Vision Science & Technology*. 9(8), 35-35 (2020).

[23] Jung, J-H., Hwang, D., Bowers, A., Peli, E. Pedestrians Collision Detection Test for Peripheral Field Loss. ARVO 2022. *Invest. Ophthalmol. Vis. Sci.*, 63 (7): 2455 – F0032 (2022).